https://doi.org/10.20965/jrm.2020.p0333

Paper:

Fabrication, Experiment, and Simulation of a Flexible Microvalve-Integrated Microarm for Microgrippers Using Electrorheological Fluid

Joon-Wan Kim*, Kazuhiro Yoshida*, Toru Ide, and Shinichi Yokota*****

*Laboratory for Future Interdisciplinary Research of Science and Technology (FIRST), Institute of Innovative Research (IIR), Tokyo Institute of Technology
4259 Nagatsuta, Midori-ku, Yokohama, Kanagawa 226-8503, Japan
E-mail: {woodjoon, yoshida}@pi.titech.ac.jp
**Department of Mechano-Micro Engineering, Interdisciplinary Graduate School of Science and Engineering, Tokyo Institute of Technology
4259 Nagatsuta, Midori-ku, Yokohama, Kanagawa 226-8503, Japan
E-mail: tooru_ide@jtekt.co.jp
***Precision and Intelligence Laboratory, Tokyo Institute of Technology
4259 Nagatsuta, Midori-ku, Yokohama, Kanagawa 226-8503, Japan
E-mail: syokota.pi2@gmail.com
[Received December 6, 2019; accepted March 18, 2020]

Because of the power density advantages of fluid power systems, many researchers have developed microactuators using homogeneous electrorheological (ER) fluids (ERFs) for applications to various micromachines. An ER valve, as a critical component of the ER actuator, can control ERF flow by the apparent viscosity increase resulting from the applied electric field without any mechanical moving parts. Hence, it is adequate for the miniaturization of a fluidic microactuator. However, it is not easy to integrate rigid ER valves into soft microrobots. To overcome these limitations, we developed a novel elastic ER microarm using flexible ER valves (FERVs) in this study. Each microarm consists of an FERV, a movable chamber, and a displacement constraint element, so that it bends with the inner pressure controlled by the FERV. We proposed and developed a micro-electromechanical system fabrication process for the FERV, movable chamber, and displacement constraint element. By utilizing the proposed method, we successfully fabricate a FERV-integrated microarm. The characteristics of the FERV were experimentally clarified. In addition, the bending motion of the FERV-integrated microarm was demonstrated by experiments and verified by finite-element method simulation. This ER microarm was shown to be feasible for an ER microgripper composed of multiple microarms.

Keywords: electrorheological fluid (ERF), microgripper, soft actuator, fluid power control, MEMS

1. Introduction

Micromachines with high power volume density have attracted great interest in new industrial and medical applications [1–4]. Although fluid-powered microactuators are very effective in applications requiring high output power by considering scaling laws [5, 6], many attempts have been made to develop piezoelectric [7, 8], electrostatic [9], electromagnetic [10], and thermal microactutors [11] for this purpose during recent decades. This trend is the reason why it is difficult to realize very small hydraulic systems (micropumps, microvalves, microcylinders, and so on) by considering the difficulties of microfabrication, microassembly, friction, wear, and leakage. Despite the difficulties in realization, we are interested in fluidic microactuators because of the potential advantage of providing high output power for microsystems [12–14].

To realize a fluidic microactuator, three approaches were used in this study: 1) micro-electromechanical system (MEMS) fabrication technology, 2) electrorheological (ER) fluid (ERF) as a functional and working fluid, and 3) an elastic fluidic microactuator.

MEMS technology is based on modified semiconductor fabrication techniques to create very small mechanical devices. Therefore, MEMS fabrication technology is an effective candidate to make small constituent parts and small overall systems without any additional assembly processes [15, 16].

The easiest way to overcome the issues of friction, wear, and leakage in fluidic microdevices is not to utilize any mechanical moving parts. For this purpose, an ERF is worth investigating. An ERF is a functional fluid that increases its apparent viscosity subjected to an electric field. There are mainly two types: a suspension ERF and a homogeneous ERF [17]. The suspended ERF has extremely fine particles that can induce the chains or clusters of particles at the applied electric field [18], so it is not desirable in a microchannel because of the clogging of particles [19, 20]. The ER fluid having the highest performance, the giant ER fluid (GERF) reported in 2003,

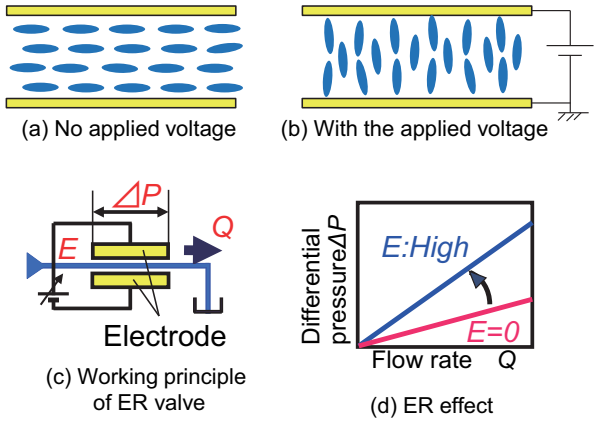

Fig. 1. Schematic diagram and working principle of an ER valve (ER effect is a phenomenon to increase the apparent viscosity when subjected to an electric field).

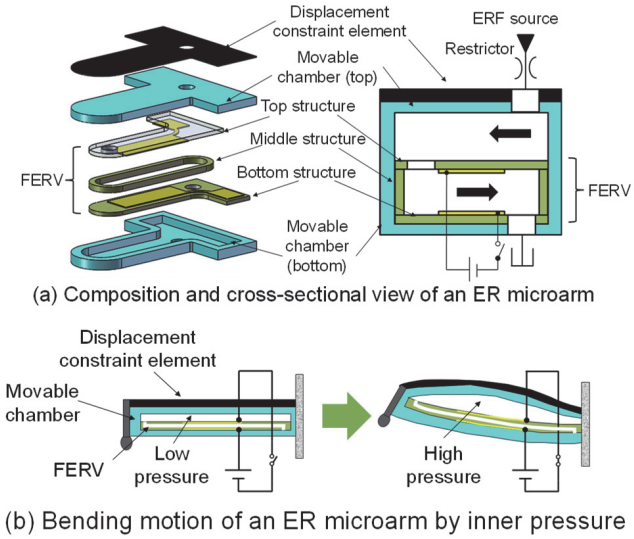

Fig. 2. Proposed ER microarm for the ER microgripper. (a) The ER microarm consists of an FERV, a movable chamber, and a displacement constraint element. The chamber pressure can be controlled by the FERV. (b) Because of a displacement constraint element, the swelling deformation by increased chamber pressure is transformed to the bending motion.

can have much higher sustainability than other ERFs, but it has a significant concern because of the use of a strong organic acid for the preparation [21]. However, a homogeneous ERF, such as a nematic liquid crystal (LC), can make its rodlike molecules rotate to the direction that increases its apparent viscosity under the electric field, as shown in **Figs. 1(a)** and **(b)**. Because of the characteristics of its ER effect and no concern about clogging, the LC was used in this study. By using the ER effect, the LC flow between a pair of parallel-plate electrodes can be easily controlled by the applied voltage, as shown in **Figs. 1(c)** and **(d)**. The flow control device is the ER valve and can be miniaturized with a simple structure without moving parts [22]. A flexible ER microvalve called as a FERV was proposed and developed for flexible and soft microactuators [23, 24]. The FERV consists of a thin cantilever structure made of SU-8 (MicroChem Corp.) for fluidic channels and thin metallic films for electrodes. Because of the thin cantilever shape and high elasticity of the plastic material (SU-8) [25, 26], the FERV can easily bend in the thickness direction because of the external force [23].

Elastic fluidic microactuators provide another method to avoid the issues of friction, wear, and leakage. They are defined as flexible or soft microactuators with at least one component that is elastically deformed by the applied pressure. Because it is challenging to fabricate low-friction microseals, microsized piston-cylinder-type microactuators are rare. However, there are no friction, wear, or sealing issues in elastic fluidic microactuators, because they do not have any sliding parts.

Based on these three approaches, a novel FERV-integrated microarm using the LC as a working ERF was developed. In this work, first, the static and dynamic characteristics of the FERV are described. Second, a microarm based on the FERV that was realized for the FERV-integrated microgripper is described. Its feasibility was investigated experimentally. Furthermore, the finite-element method (FEM) was used to compare experimental results with simulations to verify the motion of a MEMS-fabricated microarm having an FERV.

2. Concept of an FERV-Integrated Microarm for a Microgripper

Several microgrippers have been proposed using piezoelectric elements [27], shape memory alloys [28], electrothermal effects [29], electroactive polymers [30, 31], and so on. Different from the attempts mentioned above, this study focused on a MEMS-fabricated elastic ER microgripper mounted on an in-pipe working microrobot that can handle objects softly and stably for maintenance of small pipes with 10-mm diameter [24].

The ER microgripper in this study consists of two flexible ER microactuators that can perform bending motion and executes the gripping operation by installing and driving the ER microactuators in opposition. The ER microactuator constituting the gripper is referred to as an "ER microarm." The composition of the ER microarm (9.2 mm in length, 6 mm in width, and 1 mm in thickness) is shown in **Fig. 2(a)**. The ER microarm is composed of three elements: a movable chamber, a displacement constraint element, and an FERV. 1) The movable chamber is a flexible element that expands as a moving part. 2) The displacement constraint element is for converting the expansion of the movable chamber caused by the FERV-controlled pressure into a bending motion. 3) The FERV controls the internal pressure of the movable chamber. These elements are separately fabricated by MEMS technology and assembled manually. The FERV is attached to the bottom inside of the movable chamber, while the displacement constraint element adheres to the top surface of the chamber, as shown at the left of **Fig. 2(a)**.

To control the internal pressure of the ER microarm

with a sufficient pressure change, a corresponding length of the ER microvalve is required in the fluidic microchannel. If this ER microvalve is rigid [22], its rigidity interferes with the soft movement of the flexible actuator itself. However, if it is a FERV, it is possible to accommodate a long ER microvalve in the movable chamber [23]. Because of the flexibility of these three elements, it is possible to obtain bending flexibility in the thickness direction of the ER microarm. By using an external pump, the ERF is supplied into the ER microarm, as shown at the right of **Fig. 2(a)**. As shown in **Fig. 2(b)**, the FERV can control the internal pressure of the ER microarm because of the apparent viscosity change of the ERF by applying a voltage between the electrode pairs allocated in the fluidic channel in the FERV. When the internal pressure is increased, the movable chamber expands in the thickness direction. At this point, one side of the ER microarm is restricted by the displacement constraint element, generating the bending motion resulting from the geometric asymmetry, as shown in **Fig. 2(b)**. The ER microarm bends, forming an open state of the ER microgripper. By arranging these two ER microarms, an ER microgripper can be realized.

For the miniaturization of the system, it is recommended that the ER microgripper be integrated with a piezoelectric micropump as a microfluid power source. This has been proposed and developed by using the fluid inertia effect in a pipe [32]. The fabricated micropump is 2.3 cm^3 in volume and can produce fluid power up to 0.16 W for pumping viscous silicone oil, such as an ERF, which is sufficient to drive many microarms.

3. Flexible ER Microvalve (FERV)

3.1. SU-8 Cantilever-Type FERV

An FERV was developed by utilizing a negative photoresist, SU-8 (MicroChem Corp.), as a structural material. There are two main necessary conditions for the FERV: 1) flexibility and 2) controllability. For example, rubber is inadequate for the FERV, because it satisfies flexibility but not controllability. Pressurized fluidic microchannels made of rubber change the electrode gap caused by deformation, so that one cannot control pressure by using an applied voltage.

However, the epoxy resin photoresist SU-8 is a proper material for the FERV.

- Microstructures can be easily formed by SU-8 photolithographic patterning. It is suitable for manufacturing a precise microstructure with good reproducibility.

- SU-8 is a material with appropriate flexibility as a cantilever structure. The Young's modulus is reported to be between 2 and 5 GPa, as measured by experiments [25, 26]. SU-8 is softer than silicon (190 GPa) but much harder than silicone rubber (2 MPa). If a thin cantilever structure is made of SU-8, it can be bent with appropriate flexibility while maintaining the channel height without deformation by internal pressure.

- The crosslinked SU-8 is chemically stable [33]. It is highly compatible with ERF.

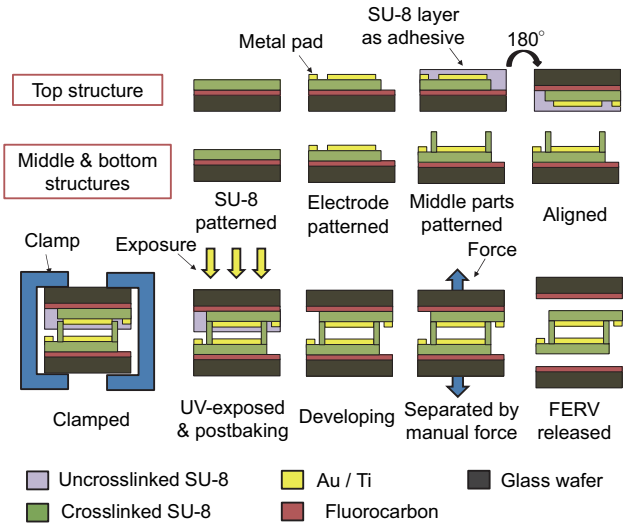

Fig. 3. Flow chart of MEMS fabrication processes of an FERV.

In this study, it was decided to utilize a two-port FERV, because the two-port one can be installed in a wider fluidic channel at the same width as the FERV, obtaining a higher flow rate with respect to the same differential pressure of the FERV. This higher flow rate can contribute to the high response of the FERV-integrated microarm.

3.2. MEMS Fabrication of FERVs

A chart of the FERV fabrication processes is shown in **Fig. 3**. Because an FERV is a complex three-dimensional structure, it is difficult to realize by two-dimensional fabrication, such as surface micromachining. First, two different wafers are fabricated independently. One has the upper electrode of the FERV on a thin SU-8 top structure, while the other has the lower electrode and the walls for fluidic channels on the thin SU-8 bottom structure. Then, these two separately fabricated wafers are bonded by non-soft-baked SU-8 as an adhesive. For testing the FERVs, it is necessary to wire the device electrically. The electrode pads on the top structure and the bottom structure are designed to be shifted with each other, so they are still open to the connection, even after bonding. The MEMS fabrication procedure with the assembly is divided into four main steps.

1) Patterning the top and bottom structures with the electrodes of the FERV.

   The first step of the FERV fabrication is almost the same process for both the upper wafer and the lower one. A fluorocarbon as a sacrificial layer is formed on the glass wafer (radio frequency power: 50 W, pressure: 225 mTorr, flow rate: 40 sccm, and discharge

Table 1. Process conditions of SU-8 patterning.

Spin coat	Revolution	Time
	500 rpm	10 s
	2000 rpm	30 s
	500 rpm	10 s
Prebake	temperature	Time
	65 °C	5 min
	95 °C	25 min
Cool down	Time	
	1 h	
Exposure	Time	
	20 s×6 times	
Cool down	Time	
	1 h	
Postexposure bake	Temperature	Time
	65 °C	2 min
	95 °C	5 min
Cool down	Time	
	1 h	
Development	Developer	Time
	SU-8 Developer	7 min

time: 10 min). Then, SU-8 is patterned to form the top and bottom structures (**Table 1**). The metal electrodes are deposited and patterned on the thin SU-8 structure by photolithography (**Table 2**) and wet chemical etching.

2) Spin-coating SU-8 for bonding to the top structure and patterning the wall of the fluidic channel on the bottom structure.

   A thin SU-8 layer is spin-coated on the upper wafer, serving as the bonding layer between two wafers. A thick SU-8 structure is patterned on the upper wafer to be the wall of the fluidic channel with the target thickness of 100 μm.

3) Bonding two wafers.

   Two wafers prepared separately are aligned and attached together. Thereafter, using the electrode pattern formed on the top structure as an ultraviolet (UV) shielding material, the SU-8 for bonding is crosslinked and connected with the channel walls on the bottom structure by UV light and postexposure baking by using the process conditions (**Table 3**). SU-8 on the electrode of the upper wafer is not exposed to UV and dissolved in developing solution, so the electrode can contact the ERF in the fluidic channel.

Table 2. Process conditions of positive photoresist (S-1805).

Spin coat	Revolution	Time
	500 rpm	10 s
	3000 rpm	30 s
	5000 rpm	0.5 s
Prebake	temperature	Time
	95 °C	120 s
Exposure	Time	
	30 s	
Postexposure bake	None	
Development	Developer	Time
	NMD-3	15 s

Table 3. Process conditions of SU-8 bonding.

Spin coat	Revolution	Time
	500 rpm	10 s
	1500 rpm	30 s
	500 rpm	10 s
Prebake	temperature	Time
	65 °C	5 min
	95 °C	15 min
Cool down	Time	
	30 min	
Prebake	temperature	Time
	80 °C	10 min
Cool down	Time	
	1 h	
Exposure	Time	
	20 s×5 times (each of top and bottom)	
Postexposure bake	Temperature	Time
	65 °C	2 min
	95 °C	5 min
Cool down	Time	
	1 h	
Development	Developer	Time
	SU-8 Developer	1 h

4) Peeling the FERV from the wafers.

   After completing the SU-8 bonding, the fabricated FERV is physically peeled from the fluorocarbon layer by using a keen utility knife (SAC-1, OLFA Corp.) and removed.

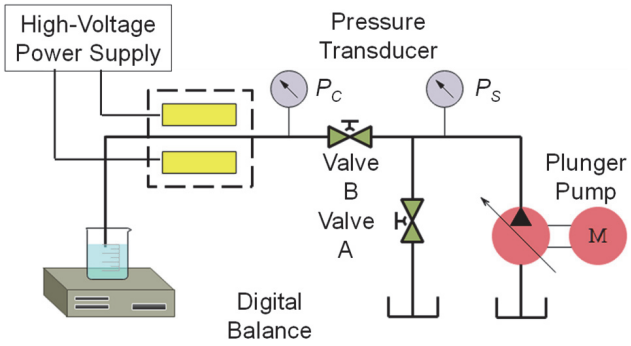

Fig. 4. Experimental apparatus for evaluating the characteristics of FERVs.

3.3. Experimental Apparatus for the FERV Characteristics

A schematic diagram of the experimental apparatus is shown in **Fig. 4**. As the working fluid, nematic liquid crystal (MLC-6457-000, Merck Ltd., Japan) was utilized as a homogeneous ERF, because it has a low base viscosity and is superior in the static and dynamic characteristics of the ER effect. As the main physical properties of MLC-6457-000, the density is 0.99×10^3 kg/m^3, and the base viscosity is 23 mPa·s. To remove the air in the pipeline of the experimental apparatus sufficiently, degassing was carried out in the vacuum chamber.

For the static characteristics of the FERV, the ER effect (κ_{ER}), which represents the ratio of the maximum viscosity at the maximum electric field to the base viscosity without the applied electric field, was utilized. The viscosity of ERF was proportional to the slope of the graph, setting flow rate on the horizontal axis and differential pressure on the vertical axis. The flow rate of the fabricated FERV was calculated from the weight of discharged ERF in unit time using the electronic balance, while the differential pressure was measured using semiconductor-type pressure sensors (KH15, Nagano Keiki Co., Ltd.).

For the dynamic characteristics of the FERV, the step response of controlled pressure was investigated when a step input of 5 kV/mm was applied. In the experimental apparatus, a large flow resistance was given by a throttle valve allocated in the upstream of the FERV to reduce the proportion of the flow rate, which was affected by the pressure change of the FERV during the experiment.

3.4. Large Model Prototype of the Two-Port FERV

Since considerable time and effort are needed to obtain the proper MEMS fabrication conditions in general, we fabricated a large model prototype to clarify the feasibility of the proposed MEMS fabrication and FERV for the ER microarm. The schematic and designed value of the large model prototype of the FERV are shown in **Fig. 5(a)**. The main dimensions are: electrode width, $B_{ER} = 0.6$ mm; electrode length, $L_{ER} = 5$ mm; and channel height, $H_{ER} = 100$ μm. The overall size was 13 mm in length, 4 mm in width, and 0.2 mm in height. It did not need delicate

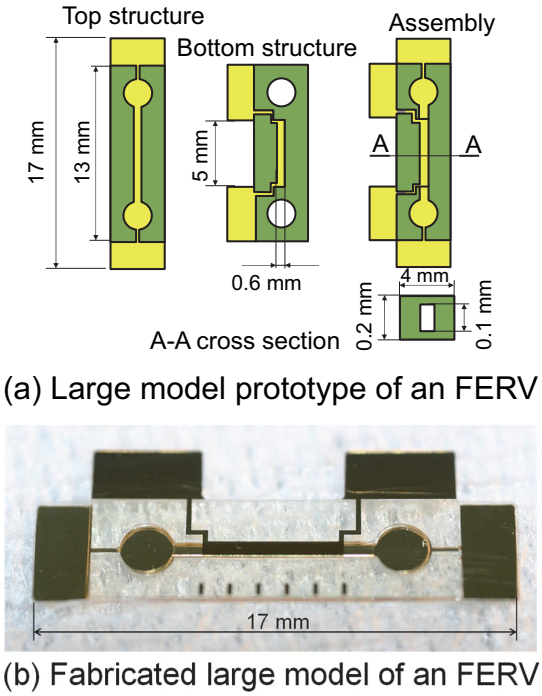

Fig. 5. Large model prototype of the FERV.

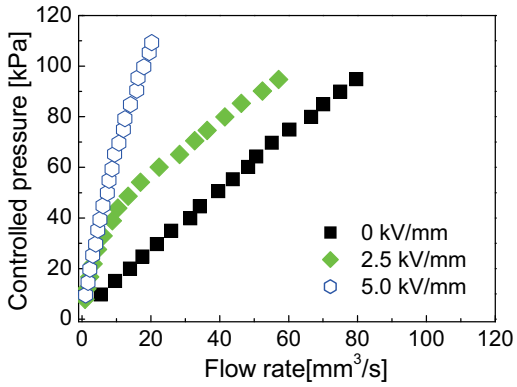

Fig. 6. Static characteristics of the large model prototype of the FERV.

fabrication conditions because of the huge bonding area between the top structure and channel wall.

By using the MEMS process shown in **Fig. 3**, the large model was successfully fabricated, as shown in **Fig. 5(b)**. The measured channel height of the fabricated large model was $H_{ER} = 128$ μm. Experiments were carried out by attaching polymer tubes (outer diameter of 4 mm and inner diameter of 2.5 mm) to the supply port and the drain port with an epoxy adhesive.

The static characteristics experiment confirmed that the fabricated large model FERV could change the valve differential pressure by the applied electric field, as previous rigid ER valves (RERVs) could. The ER effect obtained from the experimental results of this FERV was 6.2, as shown in **Fig. 6**, while the one of the RERV was 6.5. This comparison demonstrates that the ER effect is almost the same between the FERV and RERV.

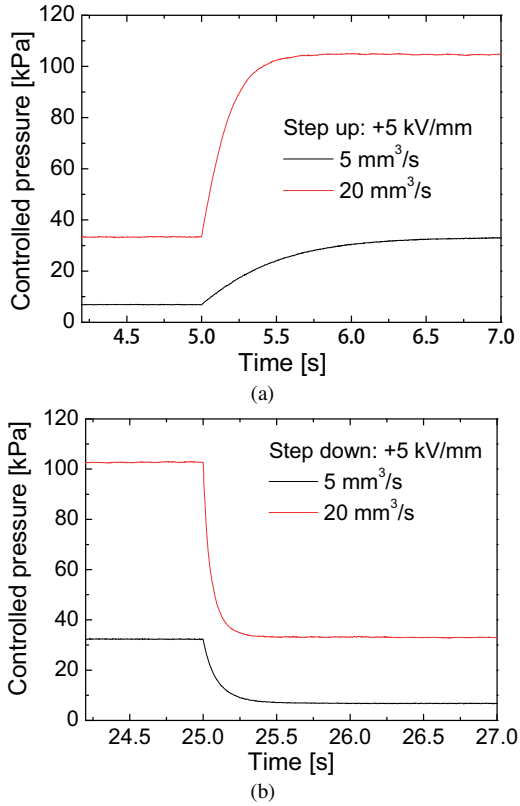

Fig. 7. Dynamic characteristics of the large model prototype of the FERV: (a) step-up response and (b) step-down response.

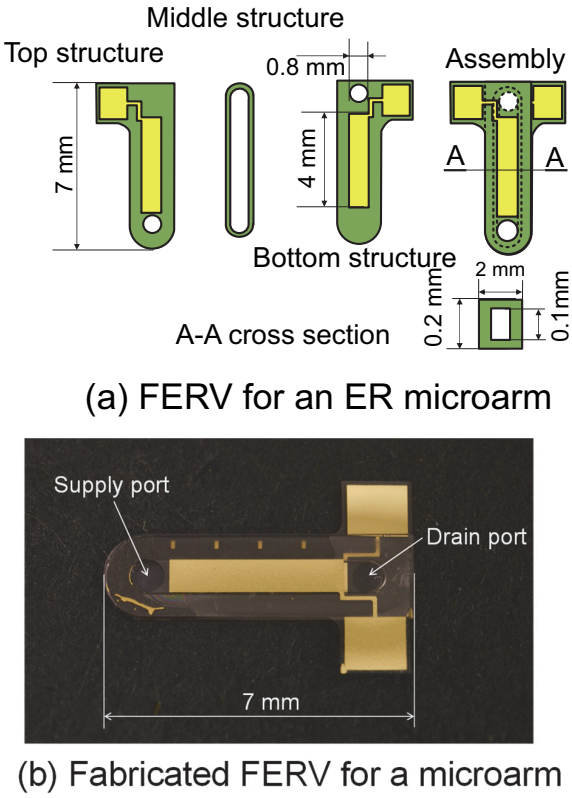

Fig. 8. Two-port FERV for the microarm and its fabricated result.

By using the same configuration of the experimental apparatus (**Fig. 4**), the differential pressure response of the FERV was measured and evaluated when a stepped electric field with an amplitude of 5 kV/mm was applied. The experimental results are shown in **Fig. 7**. The rise times for step up and down were 0.10 s and 0.06 s, respectively, with respect to a step function whose applied electric field was 5 kV/mm at a flow rate of 20 mm^3/s.

3.5. FERV for the Microarm and its Characteristics

Because the previous large model prototype of a two-port FERV (**Fig. 5**) had a total length of 17 mm and a total width of 6 mm, it was too large to apply to a soft microgripper mounted on a micromachine that works in a pipe of approximately 10-mm diameter, which is one of the promising applications of MEMS technology [24, 34]. Therefore, the size was reduced, and a two-port FERV was designed that was 7 mm in length and 2 mm in width for the flexible microgripper, as shown in **Fig. 8(a)**. If the cross-sectional area of the microchannel for the FERV becomes smaller, the flow velocity relatively increases for the same flow rate, leading to a lower ER effect. However, the lower wall height of the channel reduces the bending stiffness. Also, a larger wall width is necessary for stronger bonding between the top structure and channel wall. Setting the ER effect similar to that of a previous

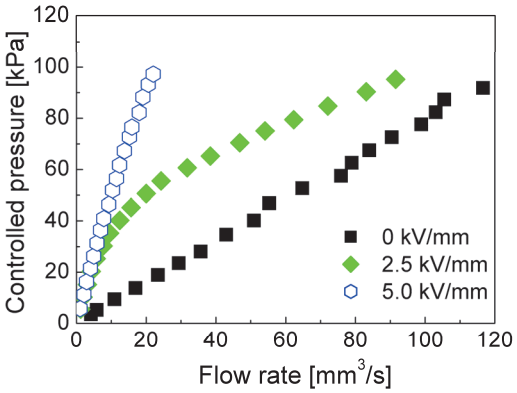

Fig. 9. Static characteristics of the two-port FERV for the microarm.

RERV ($\kappa_{ER} = 6.5$) and considering the structure, we decided to set 0.8 mm and 0.1 mm for the channel width and height, respectively. Finally, the electrode length was determined to be 4 mm as long as possible against the total length, because a shorter electrode leads to a lower ER effect.

By using the MEMS fabrication process (**Fig. 3**), the two-port FERV for the microgripper was successfully fabricated, as shown in **Fig. 8(b)**. The static and dynamic characteristics of the FERV were measured and evaluated using the experimental apparatus shown in **Fig. 4**. The measured static characteristics are shown in **Fig. 9**. No leakage of the ERF was observed, and its ER effect was

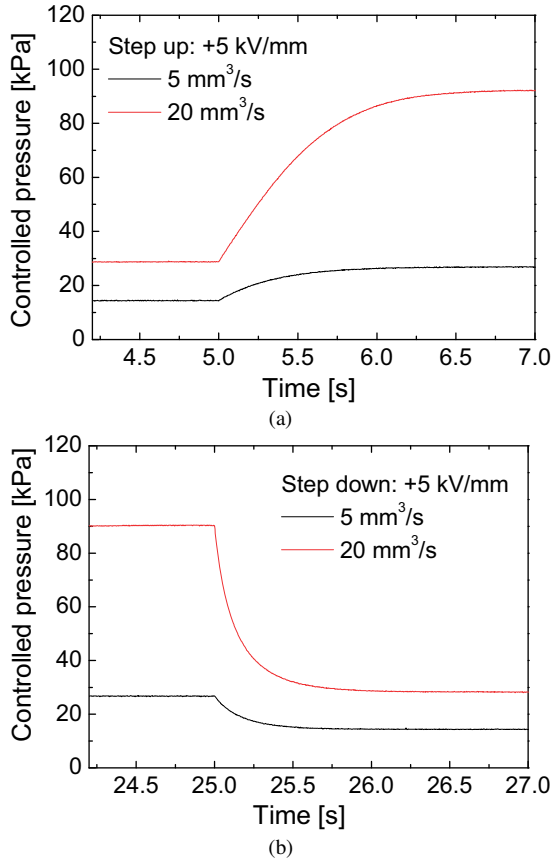

Fig. 10. Dynamic characteristics of the two-port FERV for the microarm: (a) step-up response and (b) step-down response.

6.7, which is similar to the 6.2 of the large model prototype. It was clarified that the fabricated two-port FERV can control the pressure, with the applied voltage and static characteristics normalized by the size being almost the same as the previous ones [23].

Figure 10 shows the measured step responses of the FERV when a stepped electric field with an amplitude of 5 kV/mm was applied. The rise times of step up and down were 0.23 s and 0.20 s, respectively. The reason for a slightly lower response was thought to be the residual bubbles in the hydraulic circuit, the volume of which caused it to decrease gradually as pressure increased.

4. FERV-Integrated Microarm for the ER Microgripper

4.1. Fabrication of the FERV-Integrated Microarm

A FERV-integrated microarm was designed for the ER microgripper. The movable chamber was made of polydimethylsiloxane (PDMS), which features high flexibility as a kind of silicone rubber, ease of high-precision fabrication by molding, and chemical robustness against working fluids. To realize the FERV-integrated microarm, the individually fabricated top and bottom parts were bonded with a FERV inside, as shown at the right of **Fig. 11**. A

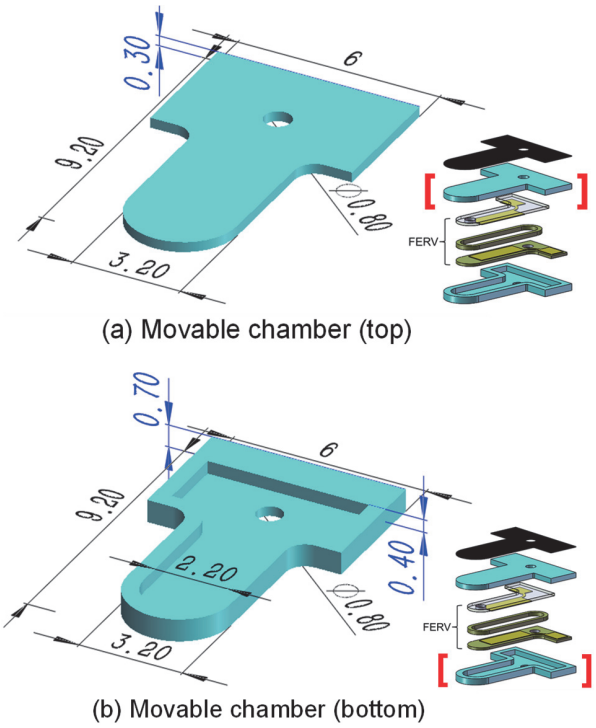

Fig. 11. Schematics and dimensions of the movable chamber.

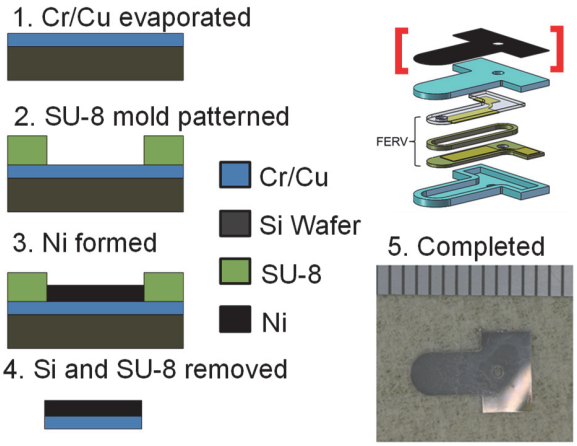

Fig. 12. MEMS fabrication process of the displacement constraint element and its fabricated result.

nickel sheet as a displacement constraint element was attached to the top of the movable chamber, as shown in **Fig. 12**.

Schematics and dimensions of the top and bottom parts of the movable chamber are shown in **Fig. 11**. The molding process based on photolithography was performed in three steps, as shown in **Fig. 13**.

1) **Micromold forming**: SU-8 layers as micromolds are patterned on wafers for the top part and the bottom one.

2) **PDMS molding**: PDMS materials are poured into the SU-8 micromolds and baked. Then, they are peeled from the wafers.

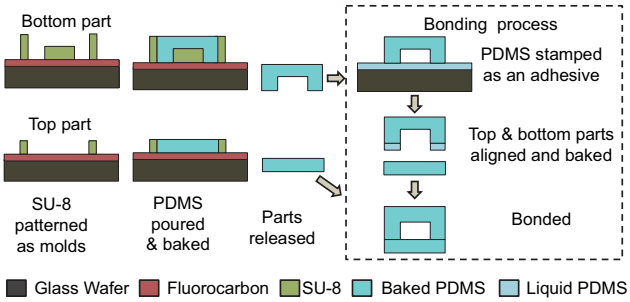

Fig. 13. MEMS fabrication process of the movable chamber.

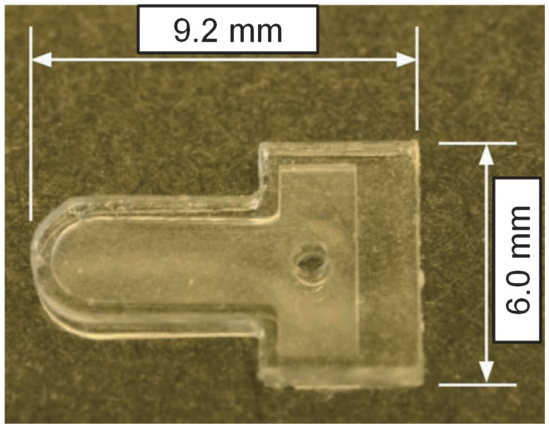

Fig. 14. Fabricated and assembled movable chamber.

3) **Bonding of the top and bottom parts for the movable chamber**: An adhesive PDMS layer is put on the bottom part. Then, the top and bottom parts are aligned, attached, and baked.

The parts were separately fabricated, and the movable chamber was successfully formed, as shown in **Fig. 14**. By using the proposed MEMS fabrication process of the nickel electroplating on the seed layer of deposited copper through the SU-8 patterned micromold, as shown in **Fig. 12**, the displacement constraint element was also successfully fabricated. The measured thickness of the displacement constraint element, as shown at the bottom right of **Fig. 12**, was 20 μm.

4.2. Characteristics of the FERV-Integrated Microarm

To investigate the leakage or tolerance, preliminary experiments using pneumatic pressure were performed, and the allowable pressure was confirmed to be higher than 100 kPa, as shown in **Fig. 15**.

The requirements of the displacement constraint element are severe and critical. The displacement constraint element should be sufficiently strong to restrain the elongation of the cantilever-shaped microarm, while it must be sufficiently flexible to prevent the bending motion. To satisfy these requirements, a thin nickel structure (20 μm in thickness) was adopted for the displacement constraint element. The Young's moduli of SU-8 and nickel are

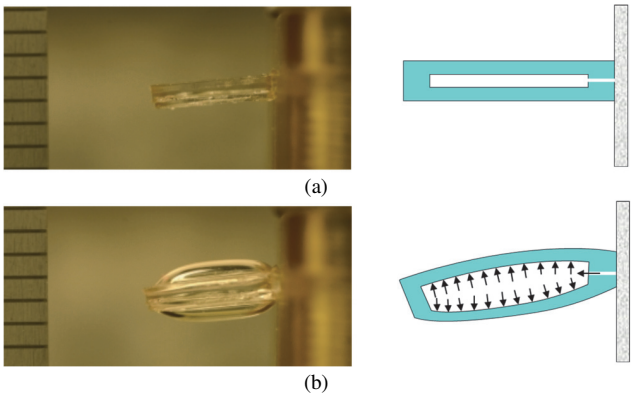

Fig. 15. Movable chamber expanded by air pressure: (a) supply pressure, 0 kPa, and (b) supply pressure, 100 kPa.

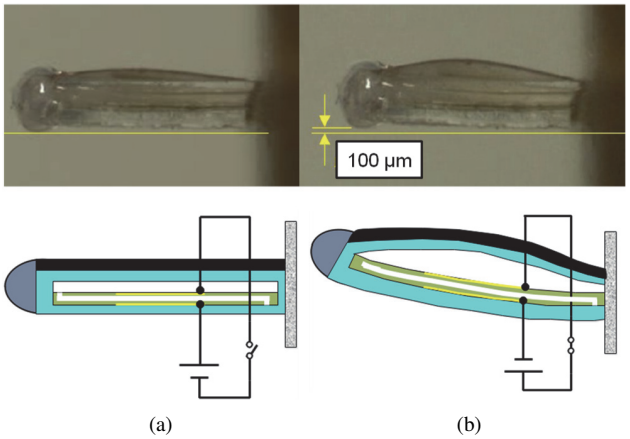

Fig. 16. Fabricated FERV-integrated microarm and its motion: (a) initial position and (b) 100 μm in bending displacement at the differential pressure of 50 kPa controlled by the FERV.

4 GPa and 200 GPa, respectively. Therefore, the calculated bending stiffness of the displacement constraint element was approximately 8% (4.3×10^{-7} Nm^2) of the FERV bending stiffness (5.1×10^{-6} Nm^2). By attaching the displacement constraint element on the movable chamber with the FERV inside, the FERV-integrated microarm was assembled. The fabricated arm and its motion are shown in **Fig. 16**. An approximately 100-μm bending displacement was obtained at a differential pressure of 50 kPa controlled by the FERV. The bending motion of the fabricated arm combined with the developed parts was successfully demonstrated.

Although this study shows the feasibility of the ER microarm, from a practical point of view, the displacement of the fabricated ER microarm is not sufficient for it to be applicable to a soft microgripper mounted on a micromachine that works in a pipe of approximately 10-mm diameter. This is the reason why the FERV made of SU-8 is harder than the PDMS movable chamber. Therefore, it is necessary to realize a novel FERV by utilizing a lower Young's modulus of materials or thinner structures.

4.3. Simulation of the FERV-Integrated Microarm

To verify the experimental result of the fabricated FERV-integrated microarm for the microgripper, FEM simulation was conducted. By applying pressure, one can acquire the simulated deflection of the FERV-integrated microarm. Assumptions were made related to the microarm: 1) the gravity is ignored and 2) the hyperplastic material of the microarm deforms elastically. Commercially available FEM software, COMSOL Multiphysics (COMSOL Inc.), was utilized to conduct the simulation. For the boundary condition, the pressure was applied to all the internal walls of the chambers.

The simulation results obtained by using the 3D model are shown in **Fig. 17**. The simulated deflection showed that the top surface profile shown in **Fig. 17(b)** of the FERV-integrated microarm was different from that of the bottom surface in **Fig. 17(c)**. The bending displacement from the experimental result was approximately 100 μm, which was similar to the simulated value shown in **Fig. 17(c)**. The good agreement between the experimental result and the simulated one shows the feasibility of the FERV-integrated microarm.

5. Conclusions

To combine the potential of high-output-power volume density in fluidic microactuators, the precision and reproducibility of MEMS fabrication technology, and the absence of wear and leakage of elastic microactuators, a soft microgripper on which an FERV is mounted was developed. The FERV-integrated microgripper consisted of multiple FERV-integrated microarms, one of which was composed of a FERV mainly made of SU-8, a movable chamber made of PDMS, and a displacement constraint element made of nickel. All components and their combined microarms were successfully fabricated by photolithography-based MEMS fabrication processes that were developed for this purpose. The demonstrated bending motion of the FERV-integrated microarm showed that the FERV-integrated microgripper is a good candidate for new industrial, biological, and medical applications that require inherent compliant behavior. Such behavior facilitates handling fragile biological tissues or even cells without damage.

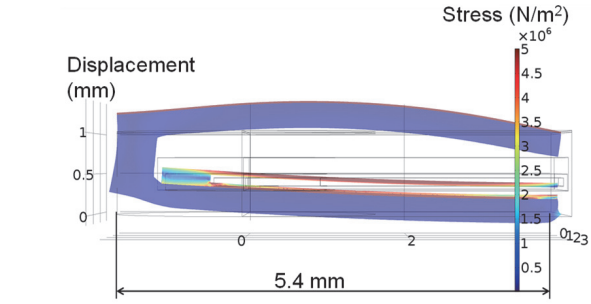

(a) Deflection of FERV-integrated microarm

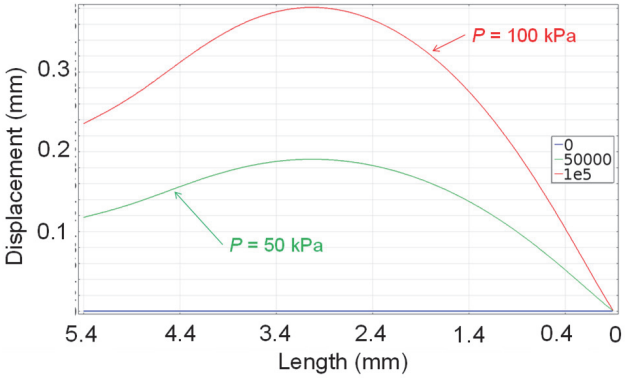

(b) Displacement of the top surface

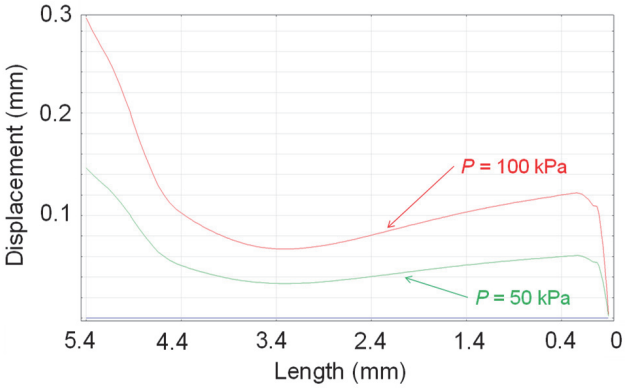

(c) Displacement of the bottom surface

Fig. 17. Simulated FERV-integrated microarm and its bending.

Acknowledgements

A part of this research was supported by a Grant-in-Aid for Scientific Research in Priority Areas, No. 16078205, of the Ministry of Education, Culture, Sports, Science and Technology of Japan.

References:

[1] M. A. Unger, H.-P. Chou, T. Thorsen, A. Scherer, and S. R. Quake, "Monolithic microfabricated valves and pumps by multilayer soft lithography," Science, Vol.288, Issue 5463, pp. 113-116, 2000.

[2] M. De Volder, J. Peris, D. Reynaerts, J. Coosemans, R. Puers, O. Smal, and B. Raucent, "Production and characterization of a hydraulic microactuator," J. of Micromechanics and Microengineering, Vol.15, No.7, pp. S15-S21, 2005.

[3] Y. Suzuki, Y. Okada, J. Ogawa, S. Sugiyama, and T. Toriyama, "Experimental study on mechanical power generation from MEMS internal combustion engine," Sensors and Actuators A: Physical, Vol.141, Issue 2, pp. 654-661, 2008.

[4] M. De Volder, F. Ceyssens, D. Reynaerts, and R. Puers, "Micro-sized piston-cylinder pneumatic and hydraulic actuators fabricated by lithography," IEEE J. of Microelectromechical Systems, Vol.18, Issue 5, pp. 1100-1104, 2009.

[5] K. Yoshida, K. Takahashi, and S. Yokota, "An in-pipe mobile micromachine using fluid power (A mechanism adaptable to pipe diameters)," JSME Int. J. Series B, Vol.43, Issue 1, pp. 29-35, 2000.

[6] B. Gorissen, D. Reynaerts, S. Konishi, K. Yoshida, J.-W. Kim, and M. De Volder, "Elastic inflatable actuators for soft robotic applications," Advanced Materials, Vol.29, No.43, 1604977, 2017.

[7] K. Uchino, "Micro Walking Machines Using Piezoelectric Actuators," J. Robot. Mechatron., Vol.1, No.2, pp. 124-127, 1989.

[8] Y. Irie, H. Aoyama, J. Kubo, T. Fujioka, and T. Usuda, "Piezo-Impact-Driven X-Y Stage and Precise Sample Holder for Accurate Microlens Alignment," J. Robot. Mechatron., Vol.21, No.5, pp. 635-641, 2009.

[9] T. Niino, S. Egawa, H. Kimura, and T. Higuchi, "Electrostatic artificial muscle: compact, high-power linear actuators with multiple-layer structures," Proc. IEEE Micro Electro Mechanical Systems An Investigation of Micro Structures, Sensors, Actuators, Machines and Robotic Systems, Oiso, Japan, pp. 130-135, 1994.

[10] M. Miyake, K. Suzumori, and K. Uzuka, "Design and Evaluation of Electromagnetic Wobble Motor," J. Robot. Mechatron., Vol.24, No.3, pp. 480-486, 2012.

[11] M. Nishida, H. O. Wang, and K. Tanaka, "Development and Control of a Small Biped Walking Robot Using Shape Memory Alloys," J. Robot. Mechatron., Vol.20, No.5, pp. 793-800, 2008.

[12] S. Yokota, "A review on micropumps from the viewpoint of volumetric power density," Mechanical Engineering Reviews, Vol.1, No.2, DSM0014, 2014.

[13] J.-W. Kim, T. V. X. Nguyen, K. Edamura, and S. Yokota, "Triangular prism and slit electrode pair for ECF jetting fabricated by thick micromold and electroforming as micro hydraulic pressure source for soft microrobots," Int. J. Automation Technol., Vol.10, No.4, pp. 470-478, 2016.

[14] J.-W. Kim, Y. Yamada, and S. Yokota, "Micro ECF (electro-conjugate fluid) hydraulic power sources based on the modular design of TPSEs (triangular prism and slit electrode pairs)," The Int. J. of Advanced Manufacturing Technology, Vol.106, Issue 1, pp. 627-639, 2020.

[15] O. C. Jeong, and S. Konishi, "Fabrication of a peristaltic micro pump with novel cascaded actuators," J. of Micromechanics and Microengineering, Vol.18, No.2, 025022, 2008.

[16] C. Moraes, Y. Sun, and C. A. Simmons, "Solving the shrinkage-induced PDMS alignment registration issue in multilayer soft lithography," J. of Micromechanics and Microengineering, Vol.19, No.6, 065015, 2009.

[17] M. De Volder, K. Yoshida, S. Yokota, and D. Reynaerts, "The use of liquid crystals as electrorheological fluids in microsystems: model and measurements," J. of Micromechanics and Microengineering, Vol.16, No.3, pp. 612-619, 2006.

[18] S. B. Choi, C. C. Cheong, J. M. Jung, and Y. T. Choi, "Position control of an er valve-cylinder system via neural network controller," Mechatronics, Vol.7, Issue 1, pp. 37-52, 1997.

[19] M. Kohl, "Fluidic actuation by electrorheological microdevices," Mechatronics, Vol.10, Issues 4-5, pp. 583-594, 2000.

[20] M. Nakano, T. Katou, A. Satou, K. Miyata, and K. Matsushita, "Three-ports micro ER valve for ER suspension fabricated by photolithography," J. of Intelligent Material Systems and Structures, Vol.13, Issues 7-8, pp. 503-508, 2002.

[21] W. Wen, X. Huang, S. Yang, K. Lu, and P. Sheng, "The giant electrorheological effect in suspensions of nanoparticles," Nature Materials, Vol.2, Issue 11, pp. 727-730, 2003.

[22] K. Yoshida, M. Kikuchi, J.-H. Park, and S. Yokota, "Fabrication of micro electro-rheological valves (ER valves) by micromachining and experiments," Sensors and Actuators A: Physical, Vol.95, Issues 2-3, pp. 227-233, 2002.

[23] J.-W. Kim, K. Yoshida, K. Kouda, and S. Yokota, "A flexible electro-rheological microvalve (FERV) based on SU-8 cantilever structures and its application to microactuators," Sensors and Actuators A: Physical, Vol.156, Issue 2, pp. 366-372, 2009.

[24] K. Yoshida, N. Tsukamoto, J.-W. Kim, and S. Yokota, "A study on a soft microgripper using MEMS-based divided electrode type flexible electro-rheological valves," Mechatronics, Vol.29, pp. 103-109, 2015.

[25] H. Lorenz, M. Despont, N. Fahrni, N. LaBianca, P. Renaud, and P. Vettiger, "SU-8: a low-cost negative resist for MEMS," J. of Micromechanics and Microengineering, Vol.7, No.3, pp. 121-124, 1997.

[26] C. J. Robin, A. Vishnoi, and K. N. Jonnalagadda, "Mechanical Behavior and Anisotropy of Spin-Coated SU-8 Thin Films for MEMS," J. of Microelectromechanical Systems, Vol.23, Issue 1, pp. 168-180, 2014.

[27] M. N. M. Zubir, B. Shirinzadeh, and Y. Tian, "Development of a novel flexure-based microgripper for high precision micro-object manipulation," Sensors and Actuators A: Physical, Vol.150, Issue 2, pp. 257-266, 2009.

[28] M. Leester-Schadel, B. Hoxhold, C. Lesche, S. Demming, and S. Buttgenbach, "Micro actuators on the basis of thin SMA foils," Microsystem Technologies, Vol.14, No.4, pp. 697-704, 2008.

[29] F. Krecinic, T. Chu Duc, G. K. Lau, and P. M. Sarro, "Finite element modeling and experimental characterization of an electro-thermally actuated silicon-polymer micro gripper," J. of Micromechanics and Microengineering, Vol.18, No.6, 064007, 2008.

[30] R. Lumia and M. Shahinpoor, "IPMC microgripper research and development," J. of Physics: Conf. Series, Vol.127, 012002, 2008.

[31] S. Guo, T. Fukuda, and K. Asaka, "A new type of fish-like underwater microrobot," IEEE/ASME Trans. on Mechatronics, Vol.8, pp. 136-141, 2003.

[32] K. Yoshida, T. Muto, J.-W. Kim, and S. Yokota, "An ER microactuator with built-in pump and valve," Int. J. Automation Technol., Vol.6, No.4, pp. 468-475, 2012.

[33] D. Han, K. Yoshida, and J.-W. Kim, "A Novel Hybrid Removal Technology for High-Aspect-Ratio SU-8 Micromolds in ECF (Electro-Conjugate Fluid) Micropumps Fabrication by UV-LIGA," J. of Microelectromechanical Systems, Vol.27, Issue 5, pp. 818-826, 2018.

[34] M. Takeda, "Applications of MEMS to industrial inspection," Technical Digest. MEMS 2001. Proc. of 14th IEEE Int. Conf. on Micro Electro Mechanical Systems (Cat. No.01CH37090), Interlaken, Switzerland, pp. 182-191, 2001.

Name:
Joon-Wan Kim

Affiliation:
Associate Professor, Laboratory for Future Interdisciplinary Research of Science and Technology (FIRST), Institute of Innovative Research (IIR), Tokyo Institute of Technology

Address:
J3-12, 4259 Nagatsuta-cho, Midori-ku, Yokohama 226-8503, Japan

Brief Biographical History:
2005- Assistant Professor, Precision and Intelligence Laboratory, Tokyo Institute of Technology
2013- Associate Professor, Precision and Intelligence Laboratory, Tokyo Institute of Technology
2016- Associate Professor, FIRST, IIR, Tokyo Institute of Technology

Main Works:
• "Tube-type micropump by using electro-conjugated fluid (ECF)," Sensors and Actuators A: Physical, Vol.174, pp. 155-161, 2012.
• "Comprehending Electro-conjugate Fluid (ECF) Jets by Using the Onsager Effect," Sensors and Actuators A: Physical, Vol.295, pp. 266-273, 2019.

Membership in Academic Societies:
• The Japan Society of Mechanical Engineers (JSME)
• The Japan Fluid Power System Society (JFPS)
• The Japan Society for Precision Engineering (JSPE)
• The Institute of Electrical and Electronics Engineers (IEEE)

Name:
Kazuhiro Yoshida

Affiliation:
Professor, Laboratory for Future Interdisciplinary Research of Science and Technology (FIRST), Institute of Innovative Research (IIR), Tokyo Institute of Technology

Address:
R2-42, 4259 Nagatsuta-cho, Midori-ku, Yokohama 226-8503, Japan

Brief Biographical History:
1989- Research Associate, Precision and Intelligence Laboratory, Tokyo Institute of Technology
1996- Associate Professor, Precision and Intelligence Laboratory, Tokyo Institute of Technology
2015- Professor, Precision and Intelligence Laboratory, Tokyo Institute of Technology
2016- Professor, FIRST, IIR, Tokyo Institute of Technology

Main Works:
• "An MEMS-based multiple electro-rheological bending actuator system with an alternating pressure source," Sensors and Actuators A: Physical, Vol.245, pp. 68-75, 2016.
• "A novel bending microactuator with integrated flexible electrorheological microvalves using an alternating pressure source for multi-actuator systems," Microsystem Technologies, Published online, doi: 10.1007/s00542-019-04685-9, 2019.

Membership in Academic Societies:
• The Japan Society of Mechanical Engineers (JSME)
• The Japan Fluid Power System Society (JFPS)
• The Robotics Society of Japan (RSJ)
• The Institute of Electrical and Electronics Engineers (IEEE)

Name:
Toru Ide

Affiliation:
Assistant Manager, JTEKT Corporation

Address:
1-1 Kotobuki-cho, Toyota, Aichi 471-0834, Japan

Brief Biographical History:
2009- JTEKT Corporation

Membership in Academic Societies:
• Japanese Society of Tribologists (JAST)

Name:
Shinichi Yokota

Affiliation:
Professor Emeritus, Tokyo Institute of Technology

Address:
4259 Nagatsuta-cho, Midori-ku, Yokohama 226-8503, Japan

Brief Biographical History:
1975- Research Associate, Research Laboratory of Precision Machinery and Electronics, Tokyo Institute of Technology
1995- Professor, Precision and Intelligence Laboratory, Tokyo Institute of Technology
2015- Professor Emeritus, Tokyo Institute of Technology

Main Works:
• "New Construction of an Electro-Conjugate Fluid-jet Driven Micromotor with Inner Diameter of 2mm," Proc. of the Institution of Mechanical Engineers (IMechE), Part I: J. of Systems and Control Engineering, Vol.220, No.4, pp. 251-256, 2006 (Donald Julius Groen Prize 2006 from IMechE).
• "A Liquid Rate Gyroscope using Electro-conjugate Fluid," Sensors and Actuators A: Physical, Vol.149, Issue 2, pp. 173-179, 2009.

Membership in Academic Societies:
• The Japan Society of Mechanical Engineers (JSME), Fellow
• The Japan Fluid Power System Society (JFPS), Fellow / Honorary Member